

Planar Robot Casting with Real2Sim2Real Self-Supervised Learning

Vincent Lim^{1,*}, Huang Huang^{1,*}, Lawrence Yunliang Chen¹, Jonathan Wang¹,
Jeffrey Ichnowski¹, Daniel Seita¹, Michael Laskey², Ken Goldberg¹

Abstract—Manipulation of deformable objects using a single parameterized dynamic action can be useful for tasks such as fly fishing, lofting a blanket, and playing shuffleboard. Such tasks take as input a desired final state and output one parameterized open-loop dynamic robot action which produces a trajectory toward the final state. This is especially challenging for long-horizon trajectories with complex dynamics involving friction. This paper explores the task of *Planar Robot Casting (PRC)*: where one planar motion of a robot wrist holding one end of a cable causes the other end to slide across the plane toward a desired target. PRC allows the cable to reach points beyond the robot’s workspace and has applications for cable management in homes, warehouses, and factories. To efficiently learn a PRC policy for a given cable, we propose *Real2Sim2Real*, a self-supervised framework that automatically collects physical trajectory examples to tune parameters of a dynamics simulator using Differential Evolution, generates many simulated examples, and then learns a policy using a weighted combination of simulated and physical data. We evaluate *Real2Sim2Real* with three simulators, Isaac Gym-segmented, Isaac Gym-hybrid, and PyBullet, two function approximators, Gaussian Processes and Neural Networks (NNs), and three cables with differing stiffness, torsion, and friction. Results on 16 held-out test targets for each cable suggest that the NN PRC policies using Isaac Gym-segmented attain median error distance (as % of cable length) ranging from 8% to 14%, outperforming baselines and policies trained on only real or only simulated examples. Code, data, and videos are available at <https://tinyurl.com/robotcast>.

I. INTRODUCTION

Although there is substantial research on learning ballistic throwing or hitting motions for rigid objects [29, 66], there is less research into learning dynamic motions to manipulate deformable objects such as cables and fabrics. Dynamics modeling in these contexts is challenging due to uncertainty in deformability, elasticity, and friction during the object’s motion. When computing a single action in this setting (without feedback control), the complexities of state estimation and dynamics modeling are compounded by the long duration for which the system evolves after the robot action. Simulation is often used to avoid collecting physical examples, which can be time-consuming and hazardous. However, overcoming the simulation to reality (Sim2Real) gap is a long-standing problem in robotics [20, 31, 40, 53], and is particularly difficult for deformable objects.

In this paper, we consider *Planar Robot Casting (PRC)*, a procedure in which a robot dynamically manipulates a cable through 2D space, as illustrated in Fig. 1. We use the generic

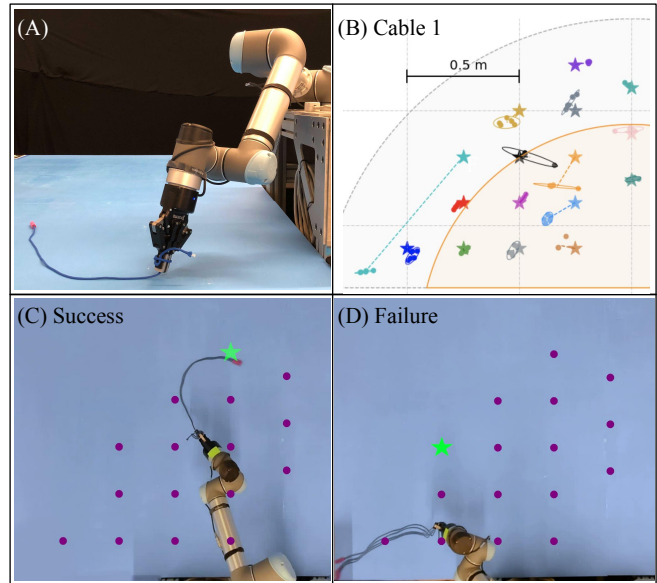


Fig. 1: In *Planar Robot Casting (PRC)*, a single planar motion of a robot wrist holding one end of a cable causes the other end of the cable to slide across the plane and stop at a desired target point, which may lie outside the robot workspace. (A) shows a side view of a UR5 robot with cable and planar workspace, (B) illustrates test performance on Cable 1 for 16 targets. The gold inner sector represents the robot workspace, while the grey outer sector represents the reachable workspace of the cable. (C,D) show multiple superimposed overhead views of the robot and cable with associated target points after PRC actions with the learned policy, in (C) an example with low error and in (D) an example with high error, in endpoint position.

term *cable* to refer to any 1D deformable object with low stiffness, such as cables, ropes, and threads. We propose *Real2Sim2Real*, a self-supervised robot learning framework that starts by collecting physical examples, uses them to tune a simulator, and then uses a combination of physical and simulated examples to train policies for PRC. As motion is restricted to a 2D plane, we do not address the 3D analog of PRC, Spatial Robot Casting (SRC), used in tasks such as fly fishing [15].

PRC is easier to visualize than SRC but can be harder to model due to inherent uncertainty about static and dynamic friction. In both PRC and SRC, the cable is infinite-dimensional and there is a long time horizon for the motion of the cable free end resulting from a motion at the controlled end. This paper contributes:

- 1) A formulation of Planar Robot Casting, with an automated reset and parameterized one-step action space.
- 2) Real2Sim2Real, a robot learning framework for efficiently learning policies for PRC.
- 3) A hardware testbed for PRC with a UR5 robot and an

*Equal contribution.

¹AUTOLAB at the University of California, Berkeley, USA.

²Toyota Research Institute, CA, USA.

overhead high-speed video camera.

- 4) Three PRC simulation environments using NVIDIA Isaac Gym and PyBullet, and application of Differential Evolution [9, 52] for efficiently tuning simulation parameters based on a small set of physical examples.
- 5) Data from 64,350 simulated experiments and 2,076 physical experiments with 3 distinct cables.
- 6) Analysis comparing simulators, function approximators, and datasets, suggesting that Real2Sim2Real can efficiently learn PRC control policies that reach target positions within 15% of cable length, even when targets are outside the reachable workspace of the robot.

II. RELATED WORK

A. Deformable 1D Object Manipulation

Manipulation of 1D deformable objects such as cables has a long history in robotics; see Sanchez *et al.* [47] for a recent survey. Some representative applications include surgical suturing [35, 49], knot-tying [5, 17, 36, 57], untangling ropes [16, 28], deforming wires [39], inserting cables into receptacles [51, 58], and playing diablo [11].

There is recent interest in using learning-based techniques for manipulating cables, often with pick-and-place actions and quasistatic dynamics, so that the robot deforms the cable while allowing it to settle between actions. This can be combined with learning from demonstrations [48, 65] and self-supervised learning [38, 41]. Prior work has also used quasistatic simulators [24] to train cable manipulation policies using reinforcement learning (RL) for transfer to physical robots [59, 64]. However, as we show in Sec. V, there are limits in the free-end reachability of such quasistatic procedures, motivating high-speed, dynamic motions.

B. Simulator Tuning for Sim2Real

Sim2Real transfer has emerged as an effective technique wherein a robot can learn a policy in simulation and then transfer it to the real world, but this can suffer from the mismatch between simulation and real [20]. Hence, one option for Sim2Real is to perform traditional system identification [26] to tune a simulator to match real-world data, but this may be challenging with the infinite-dimensional configuration spaces of cables. An alternative is to use domain randomization over vision [46, 53] or dynamics [42] parameters in simulation. A drawback is that too much randomization can hinder policy training [34] and that researchers must estimate suitable ranges for parameters to randomize. This has motivated work on interleaving policy training using RL in simulation and tuning simulators with real-world data [8, 12]. Recently, Chang and Padir [7] proposed a Sim2Real2Sim pipeline for cable unplugging where the Sim2Real step determines grasp points, and the Real2Sim step uses sensors to update a cable model in simulation. Similarly, we tune a simulator, but do not require repeated iterations of collecting real-world data with simulator tuning, and we train policies using supervised learning and do not need to use potentially brittle RL algorithms [1, 18]. Furthermore, unlike Chang and Padir, we do not require

cable sensors and we use the tuned simulator to improve the performance of the physical robot.

C. Dynamic Manipulation

In dynamic manipulation, a robot executes rapid actions to quickly move objects to desired configurations [33]. In early work, Lynch and Mason [29] study planar dynamic manipulation primitives such as snatching, throwing, and rolling, and Ruiz-Ugalde *et al.* [45] build a physics-based model of pushing actions so that a robot can slide objects into a desired pose. More recent work has introduced robots that can catch items by predicting item trajectories [21], toss arbitrary objects via self-supervised learning [66], and swing items upwards using tactile feedback [55]. As with these works, we use dynamic motions, but focus specifically on cable manipulation. Furthermore, we use a tuned simulator to accelerate learning and do not require tactile sensing.

D. Dynamic Manipulation of Deformable Objects

Researchers have developed several analytic physics models to describe the dynamics of moving cables. For example, Gatti-Bonoa *et al.* [15] present a 2D dynamic model of fly fishing. They model the fly line as a long elastica and the fly rod as a flexible Euler-Bernoulli beam, and propose a system of differential equations to predict the movement of the fly line in space and time. In contrast to continuum models, Wang *et al.* [56] propose using a finite-element model to represent the fly line by a series of rigid cylinders that are connected by massless hinges. In contrast to these works, we evaluate on physical robots.

For robotic dynamic-cable manipulation, Yamakawa *et al.* [60–63] show that a high-speed manipulator can tie knots using snapping motions. They simplify the modeling of cable deformation by assuming each cable component follows the robot end-effector motion with constant time delay. Kim *et al.* [22] study a mobile robot system with a cable attached as a tail that can strike objects. They use a Rapidly-exploring Random Tree (RRT) [23] and a particle-based representation to address the uncertainty in state transition. In contrast, we aim to control cables for tasks in which we may be unable to rely on assumptions in [22, 61] for cable motion.

In closely related prior work, Zhang *et al.* [67] propose a self-supervised learning technique for dynamic manipulation of fixed-end cables for vaulting, knocking, and weaving. They parameterize actions by computing a motion using a quadratic program and learning the apex point of the trajectory. In contrast, we use free-end cables. Zimmermann *et al.* [68] study the dynamic manipulation of deformable beams and cloth in the free-end setting. They model elastic objects using the finite-element method [4] and use optimal control techniques for trajectory optimization. They study whipping a beam so that its free end hits a predefined target with maximum speed. The simulated motions perform well in real for simple dynamical systems such as a pendulum, but performance deteriorates for complex soft bodies due to the reality gap. We develop a learned, data-driven approach for robotic manipulation of free-end cables and focus on PRC.

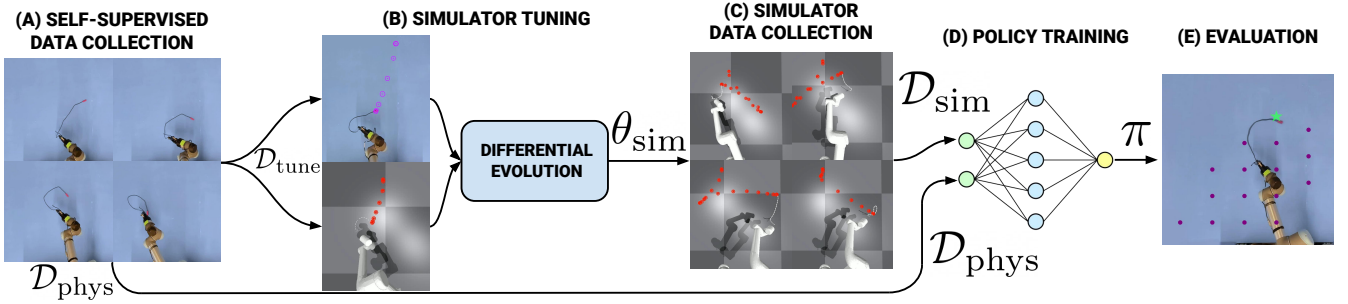


Fig. 2: The *Real2Sim2Real* pipeline for PRC. We collect a physical dataset $\mathcal{D}_{\text{phys}}$ (A) in a self-supervised manner. We subsample $\mathcal{D}_{\text{phys}}$ to generate $\mathcal{D}_{\text{tune}}$, and use it to tune simulation parameters so that its trajectories match real trajectories using Differential Evolution (B), then use the tuned simulator to generate a large dataset \mathcal{D}_{sim} (C). We use a weighted combination of \mathcal{D}_{sim} and $\mathcal{D}_{\text{phys}}$ to train the policy (D) and evaluate the policy in real (E).

III. PROBLEM STATEMENT

In Planar Robot Casting, a robot gripper holds a cable at one endpoint and swings it along a planar surface with a single continuous motion so that the other endpoint comes to rest at a target s_d . The held cable endpoint is at polar coordinate $s = (r, \theta)$, with the robot base at the origin. The objective is to find a per-cable policy π that minimizes the expected error $\|s_{f,c} - s_{d,c}\|_2$, where $s_{f,c}$ is the final state and $s_{d,c}$ is s_d in Cartesian coordinates. We assume that the s_d is reachable by the cable endpoint (see Fig. 1).

IV. METHOD

To learn a policy that accounts for variations in cable properties such as mass, stiffness, and friction, we propose a *Real2Sim2Real* (R2S2R) framework (Fig. 2) and apply it to PRC. To support this framework, we define a reset procedure to bring the system into a consistent starting state and a parameterized trajectory function that generates a dynamic arm action. The first step of R2S2R autonomously collects physical trajectories, and the second step tunes a simulator to match the physical environment. R2S2R then uses the tuned simulator to generate simulated trajectories, and combines the simulated and physical datasets to train a policy.

A. Reset Procedure

To automate data collection and bring the cable into a consistent starting state before each action, we define a 5-step reset procedure, in which the robot (1) lifts the cable up with the free-end touching the surface to prevent the cable from dangling; (2) continues to lift the cable such that the free-end is just above the surface; (3) hangs still for 3 seconds to stabilize; (4) swings the cable out of the plane, so that the cable straightens along the center axis of the surface and lands with its endpoint far from the robot base; and (5) slowly pulls the cable towards the robot to the reset position $(r_0, 0)$. The project website illustrates the reset procedure.

B. Parameterized Actions

To generate quick, smooth, dynamic actions that are low dimensional, thus facilitating data generation and training, we define a parameterized action composed of two sweeping arcs (Fig. 3):

$$\mathbf{a} = (\theta_1, r_1, \theta_2, r_2, \alpha, v_{\text{max}}). \quad (1)$$

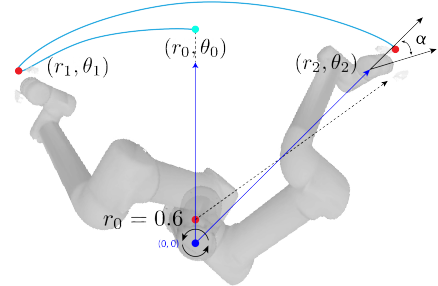


Fig. 3: Example of a spline trajectory traced by the end effector of the UR5 for $r_0 = 0.6$. The reset procedure brings the end effector to $(r_0, 0)$ and the motion is smoothly interpolated along one spline to (r_1, θ_1) , then along a second spline to (r_2, θ_2) . Along the second spline, an offset α is added to the wrist joint angle produced by the IK solver.

The motion starts at $(r_0, 0)$, arcs to (r_1, θ_1) , and arcs back to (r_2, θ_2) . In the motion, α is the wrist joint rotation about the z -axis during the second arc, and v_{max} is the maximum velocity. This parameterization is motivated by observing human attempts at the PRC task.

We convert action parameters to a trajectory in polar coordinates using a cubic spline to smoothly interpolate the radial coefficient from r_0 to r_2 , and use a maximum-velocity spline to interpolate the angular coefficient from 0 to θ_1 and from θ_1 to θ_2 , with maximum velocity v_{max} . The maximum-velocity spline uses a jerk-limited bang-bang control, having observed that the UR5 has difficulty following trajectories with high jerk [19]. We assume a direction change between the two arc motions, so the angular velocity at θ_1 is 0. We use an analytic inverse kinematics (IK) solver to convert the splines to joint configurations. The execution for each trajectory is about 22 seconds, including 20 seconds for the reset motion and 2 seconds for the planar motion.

This parameterization enables state symmetry. For all datasets, we sample actions such that $\theta_1 > 0$, $\theta_2 < 0$, and $\alpha \geq 0$, to obtain targets on the left of the workspace axis of symmetry. If $(\theta_1, \theta_2, r_2, \alpha, v_{\text{max}})$ produces target (r_d, θ_d) , $(-\theta_1, -\theta_2, r_2, -\alpha, v_{\text{max}})$ will produce $(r_d, -\theta_d)$. Thus, we do not evaluate targets on the right of the axis of symmetry.

C. Self-Supervised Physical Data Collection

For the first step of R2S2R, we autonomously collect a physical dataset $\mathcal{D}_{\text{phys}}$ and take a subset of $\mathcal{D}_{\text{phys}}$ to form a simulator tuning dataset $\mathcal{D}_{\text{tune}}$ to perform system

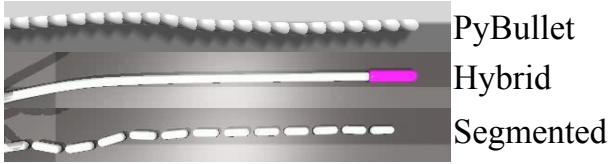


Fig. 4: Three cable simulation models for Real2Sim tuning. From top to bottom: the PyBullet model consists of capsule rigid bodies connected by 6 DOF spring constraints. The hybrid model is a soft-body rod connected to a capsule rigid body at the endpoint. The segmented model also consists of a string of capsule rigid bodies, but is connected using ball joints.

identification in simulation (Sec. IV-E). To create $\mathcal{D}_{\text{phys}}$, we grid sample each action parameter to generate $5 \times 5 \times 5 \times 4 \times 2$ trajectories, then filter it such that each trajectory abides by joint limits and is collision-free, to generate $|\mathcal{D}_{\text{phys}}| = 522$ trajectories.

For automatic data labeling, we record each trajectory using a camera and use contour detection in OpenCV [6] to track a brightly colored endpoint. We extract the 2D waypoint location $p_t = (x_t, y_t)$, where t is the timestep, every 100 ms from the start of the robot’s trajectory. For each trajectory m_j in $\mathcal{D}_{\text{phys}}$, the number of waypoints collected is $K_j = \lfloor T_j/100 \rfloor$, where T_j is the duration of m_j in milliseconds.

D. Three Simulation Models for Robot Casting

R2S2R then tunes a simulator so that it can generate data to augment policy training. We first consider which simulator and model best match real from 3 options: PyBullet [10] and two versions of NVIDIA Isaac Gym [32]. We set simulated cable geometry (e.g., length and radius), to match the real cable. Fig. 4 shows a visual comparison, and the project website provides details.

PyBullet is a CPU-based deterministic rigid-body physics simulator used in prior work on deformable object manipulation [34, 48]. We model the cable as a string of capsule-shaped rigid bodies with 6-DOF spring constraints between each consecutive pair. We tune ten parameters: twist stiffness, bend stiffness, mass, lateral friction, spinning friction, rolling friction, endpoint mass, linear damping, angular damping, and dynamic friction.

NVIDIA Isaac Gym is a GPU-based robotics simulation platform that supports the FleX [30] particle-based physics simulator designed for deformable objects and rigid bodies. We test two simulation models for the cable: a *segmented* model and a *hybrid* model, both using FleX. The segmented model is a string of 18 capsule-shaped rigid bodies with consecutive pairs linked together by a ball joint. To model cable stiffness, we tune the joint friction, cable mass, endpoint mass, and planar friction to capture variation in each respective parameter in real. The hybrid model has the same rigid endpoint from the segmented model, but the rest of the cable is a soft-body rod. We tune the Young’s modulus of the soft-body rod to model both the cable stiffness and elasticity, dynamic friction of the ground plane, and rigid endpoint mass to capture variations in friction and endpoint properties.

E. Simulator Parameter Tuning for \mathcal{D}_{sim} collection

To tune the parameters of each simulator so that simulated and real trajectories closely match, we employ a consistent protocol. Following system identification [26], the protocol uses physical trajectories from $\mathcal{D}_{\text{tune}}$ (Sec. IV-C) to minimize the discrepancy between simulated and real trajectories. We define the simulation tuning objective as finding simulation parameters that minimize the average L^2 distance between the cable endpoint in simulation \hat{p}_t to the target endpoint p_t over all trajectory timesteps, averaged over a batch of trajectories. We call this metric the average waypoint error.

As the simulation models may have parameters that have no physical analog, such as the joint friction in the segmented model, or have parameters that do not act similarly to their physical counterparts [27], we choose tuning algorithms that make no assumptions about the underlying dynamics model. We evaluate two tuning algorithms, Bayesian Optimization (BO) and Differential Evolution (DE), both of which are derivative-free black box optimization methods.

Bayesian Optimization builds a probabilistic surrogate model and uses an acquisition function that leverages the uncertainty in the posterior to decide where to query next [14]. BO has been used in policy search for RL hyperparameters [25, 50], and for tuning simulation fluid dynamics [27]. Differential Evolution is an evolutionary population-based stochastic optimization algorithm widely used for global optimization of nondifferentiable, multi-modal, and nonlinear objectives [52]. DE maintains a population of candidate solutions at each iteration and generates new candidates by combing each population member with another mutated population candidate member. It then evaluates the fitness of the trial candidates to update the population of candidate solutions until convergence. Prior work has shown DE to be effective at simulation parameter tuning [9].

We evaluate each algorithm via Sim2Sim tests. Using a fixed set of simulation parameters, we generate a small dataset of trajectories to tune randomly initialized simulators to test the effectiveness of DE and BO. We consider the discrepancy between ground truth and predicted simulation parameters and average waypoint error (see results in Sec. V-A). We then tune the simulator parameters for each simulation model to the physical data using the best performing tuning algorithm. We tune the simulator using the same process but with *physical* trajectories from $\mathcal{D}_{\text{tune}}$.

F. Size of Simulator Tuning Set $\mathcal{D}_{\text{tune}}$

We subsample 20 trajectories from $\mathcal{D}_{\text{phys}}$ to generate dataset $\mathcal{D}_{\text{tune}}$. We evaluated whether increasing the size of $\mathcal{D}_{\text{tune}}$ would reduce the discrepancy between simulation and real using a test set of 30 random physical trajectories not in $\mathcal{D}_{\text{phys}}$. We observed negligible difference in test errors between using 20 and 60 trajectories, but the latter would require $2 \times$ as long to tune on the hybrid and PyBullet models. Tuning with $|\mathcal{D}_{\text{tune}}| = 20$ trajectories did not lead to a significant speedup in the segmented model, therefore we held this value fixed.

After tuning, R2S2R generates training data \mathcal{D}_{sim} by grid sampling θ_1 , θ_2 , r_2 , ψ , and v_{max} to generate $15 \times 15 \times 15 \times 10 \times 2$ values for each respective parameter. We then filter out any trajectories that violate joint limits or with collisions to generate $|\mathcal{D}_{\text{sim}}| = 21,450$ (a, s) simulated trajectories.

G. Policies

1) *Forward Dynamics Model*: There is multi-modality between a target endpoint \mathbf{s} and valid actions \mathbf{a} , so we do not learn a policy that directly predicts a given \mathbf{s}_d . Instead, we learn a forward dynamics model f_{forw} that predicts \mathbf{s} given \mathbf{a} , and interpolates to select an action. We parameterize f_{forw} using a fully connected neural network. Given a dataset \mathcal{D} of (a, \mathbf{s}_f) trajectories, the neural network learns to predict \mathbf{s}_f given \mathbf{a} via supervised regression using MSE. During evaluation, the policy π grid samples 67,500 input actions \mathbf{a} to form a set \mathcal{A} of candidate actions. It then passes each action through the forward dynamics model f_{forw} , which outputs the predicted endpoint location (\hat{x}, \hat{y}) in Cartesian space. Given a target endpoint \mathbf{s}_d (in polar coordinates), the action $\mathbf{a} = \pi(\mathbf{s}_d)$ selected is the one minimizing the Euclidean distance between the predicted endpoint \mathbf{s}_f and the target endpoint \mathbf{s}_d :

$$\pi(\mathbf{s}) = \arg \min_{\mathbf{a} \in \mathcal{A}} \|\mathbf{s}_{f,c} - \mathbf{s}_{d,c}\|_2, \quad (2)$$

where $\mathbf{s}_{f,c}$ and $\mathbf{s}_{d,c}$ are \mathbf{s}_f and \mathbf{s}_d in Cartesian coordinates respectively.

2) *Baseline Policies*: We consider two alternative policies:

Cast and Pull. Given a target cable endpoint location $\mathbf{s}_d = (r_d, \theta_d)$, first perform a casting motion that causes the free endpoint to land at (r, θ_d) . To perform this motion, the robot rotates θ_d radians, and executes the rotated reset motion as in Sec. IV-A. After the casting motion, the robot slowly pulls the cable toward the base for a distance of $r - r_d$. The robot arm is limited to a minimum r coordinate of $r_{\text{min}} = 0.55$ to prevent the end effector from hitting the robot’s supporting table, where r_{min} is the distance from the center of the robot base to the edge of the table, limiting the reachable workspace.

Forward Dynamics Model learned with Gaussian Process. As a learning baseline, we use Gaussian Process (GP) regression [37, 44]. Using $\mathcal{D}_{\text{phys}}$, we train a GP regressor to predict the cable endpoint location \mathbf{s}_f given input action \mathbf{a} . As with the neural network forward dynamics model, we grid sample 67,500 input actions and select the trajectory that minimizes the predicted Euclidian distance to the target.

V. EXPERIMENTS

We evaluate the R2S2R pipeline on PRC with 3 cables (Fig. 5) using a physical UR5 robot (Fig. 1). The working surface is a 2.45 m wide and 1.55 m tall masonite board, painted blue and sanded to create a consistent friction coefficient across the surface. We record observations from an overhead Logitech Brio 4K webcam recording 1920×1080 images at 60 frames per second.

We define π_3 as a forward dynamics model trained on a small real dataset $\mathcal{D}_{\text{phys}}$ and π_2 as a forward dynamics model



Fig. 5: Three cables used in physical experiments. Cable 1 is a thin blue paracord, Cable 2 is a nylon cable, and Cable 3 is a thick jump rope. Each endpoint has an attached mass. The respective cable lengths are 0.63 m, 0.65 m, and 0.65 m, the respective masses are 8 g, 50 g, and 45 g, and the respective radii are 4.5 mm, 10 mm, and 14 mm.

Sim. Model	Cable 1		Cable 2		Cable 3	
	Wayp.	Last	Wayp.	Last	Wayp.	Last
PyBullet	29%	28%	28%	28%	23%	17%
Isaac Gym Hybrid	14%	23%	11%	14%	11%	13%
Isaac Gym Segm.	9%	13%	8%	9%	11%	13%

TABLE I: Error for simulators tuned using DE on a set of 30 test trajectories for 3 cables (see Fig. 5). The two metrics are the median final L^2 -distance, which is the 2D Euclidean distance between endpoint locations in simulation and reality after a trajectory terminates, and average waypoint (“Wayp.”) error. Values are expressed in percentages of cable length.

trained on a large simulated dataset \mathcal{D}_{sim} . We define π_1 as a forward dynamics model trained on the combined dataset $\mathcal{D}_{\text{phys}} \cup \mathcal{D}_{\text{sim}}$, but since $|\mathcal{D}_{\text{sim}}| \gg |\mathcal{D}_{\text{phys}}|$, we 1) upsample $\mathcal{D}_{\text{phys}}$ by randomly duplicating samples such that the real data make up 30-40% of the combined dataset to force the model to learn more from the real data, and 2) weight the loss function so that samples from $\mathcal{D}_{\text{phys}}$ are weighted higher.

A. Comparing Tuning Methods

To test the effectiveness of BO and DE for tuning the Isaac Gym simulators, we generate simulated data for several hybrid models and segmented models with arbitrarily chosen parameters. We then apply BO and DE to tune the respective simulator model parameters. For BO, we use the GPy-Opt [3] library, and test three acquisition functions: Expected Improvement (EI), Lower Confidence Bound (LCB), and Maximum Probability of Improvement (MPI). We use DE as implemented in SciPy [54]. With 5 tuning trajectories, EI performs better than LCB and MPI. The tuning errors using BO range from 3.39% to 17.98% for the hybrid model and 1.09% to 9.25% for the segmented model. DE consistently tunes the parameters to within 1% of the ground truth parameters for both the hybrid and segmented models, thus we use DE for all further simulator tuning results.

B. Real2Sim

Table I reports the Real2Sim simulator tuning results using DE. We observe that the segmented model consistently outperforms the PyBullet and hybrid models in minimizing the discrepancy between simulation and real. We attribute the larger errors of the hybrid model to the Young’s modulus parameter’s effect on the cable stiffness and elasticity. We find that the tuning algorithms reduce the value of Young’s modulus to decrease cable stiffness, which causes the cable to stretch along the length of the cable, an effect we did not observe in real. We attribute the PyBullet model performance to spring-system simulation instability associated with high

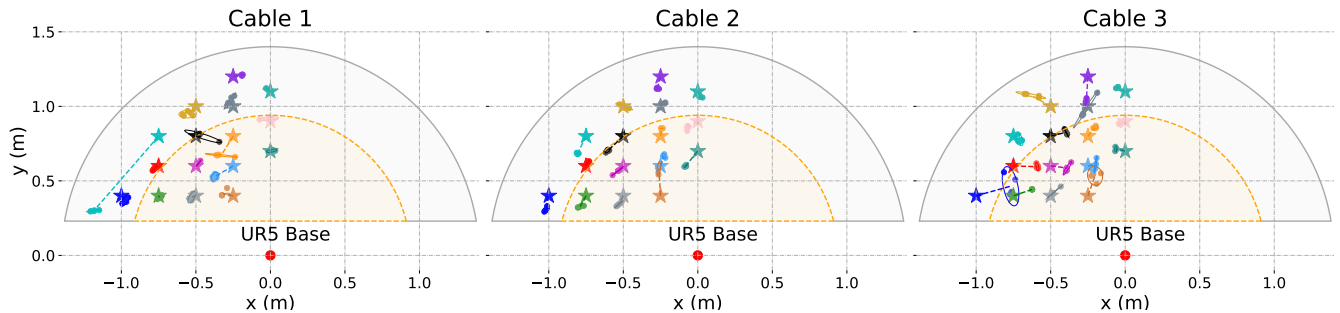


Fig. 6: Evaluation results for π_1 for each cable. The inner orange shaded region represents the robot workspace and the outer grey shaded region represents the cable workspace. The colors represent each of 16 target locations, and resulting endpoints for 5 trials per target, with associated 95% confidence ellipses. The dashed lines connect the center of each ellipse to the target point representing the mean error in position.

Model	Median	1st Quartile	3rd Quartile	Min	Max
Cast and Pull	61%	38%	86%	6%	124%
Gaussian Proc., $\mathcal{D}_{\text{phys}}$	27%	9%	51%	4%	97%
$\pi_3 (f_{\text{forw}}, \mathcal{D}_{\text{phys}})$	15%	11%	21%	8%	36%
$\pi_2 (f_{\text{forw}}, \mathcal{D}_{\text{sim}})$	14%	10%	17%	6%	115%
$\pi_1 (f_{\text{forw}}, \mathcal{D}_{\text{phys}} \cup \mathcal{D}_{\text{sim}})$	8%	5%	12%	2%	105%

TABLE II: Physical evaluation results on Cable 1, of the 2 baselines and the dynamics model f_{forw} trained on three different datasets. All errors are expressed as a percentage of cable length (0.65 m).

Cable	Median	1st Quartile	3rd Quartile	Min	Max
Cable 1	8%	5%	12%	2%	105%
Cable 2	12%	8%	16%	4%	28%
Cable 3	14%	9%	23%	6%	38%

TABLE III: Physical evaluation results of 3 cables (see Fig. 5) with 16 target positions per cable, using policies trained according to π_1 . All errors are expressed as percentages of cable length.

spring forces, particularly when preventing the cable from stretching along the length of the cable.

For cable 3, we observe that the hybrid and segmented models perform similarly. Since cable 3 is stiffer, DE produces higher Young’s modulus values that both make the simulated cable stiffer and cause it to stretch less along its length, both of which are desired properties.

While the errors for cable 2 are below 10%, we observe that cables 1 and 3 are harder for each simulator to model, each with a 4% higher last endpoint error for the segmented model. This may be due to plastic deformation in cables 1 and 3, as we observed that slight bends in the cables would remain until manually straightened by a human operator. We generate \mathcal{D}_{sim} using the segmented model, which requires approximately 4.5 minutes using 4 NVIDIA V100s.

C. Physical Experiments

As summarized in Table II, we evaluate PRC policies π_3 , π_2 , and π_1 on cable 1, as well as two baseline policies.

1) *Baseline Policies*: The analytic “Cast and Pull” baseline performs the worst out of any of the policies, as the robot would collide with the base for targets near the base. The GP trained on $\mathcal{D}_{\text{phys}}$ has substantially worse median, 3rd quartile, and maximum errors, but slightly outperforms π_3 in minimum and 1st quartile errors.

2) *Forward Dynamics Models*: We find that policies π_3 and π_2 have similar median and first and third quartile

errors, but π_2 has a substantially higher maximum error, corresponding to trajectories where the simulator has high tuning error. As the simulator is tuned with only 20 trajectories, compared to the over 500 trajectories used to train π_3 , we achieve similar evaluation performance while using 96% fewer physical trajectories. When we combine the two datasets to train π_1 , the median error drops by nearly 50%. However, the maximum error rose to above 100% for a single target, suggesting that while the combined dataset substantially improves overall results, it may introduce outliers in regions of the workspace where the simulator is unable to match reality.

Given that π_1 performs the best out of the policies, we proceed to evaluate the performance for 3 cables on 16 target positions using policy π_1 trained for each cable separately, and repeat each action 5 times per target. Results are summarized in Table III. We quantify the aleatoric uncertainty with the 95% confidence ellipses in Fig. 6.

We attribute the epistemic uncertainty to two sources: the Sim2Real gap, where trajectories executed in simulation do not accurately reflect real, and the learning error in the forward dynamics model. The results suggest that the R2S2R pipeline can apply to other cables.

VI. CONCLUSION AND FUTURE WORK

In this paper, we present Real2Sim2Real, a self-supervised learning framework, and apply it to Planar Robot Casting. Experiments suggest that the framework, which collects physical data, tunes a simulator to match the physics of the real data, and trains policies from a weighted combination of real and simulated data, can achieve an error between 12% and 15% on the PRC task. The self-supervised fine-tuning process relies on executing hundreds of trajectories in the physical setup, which may be infeasible in other dynamic manipulation domains. Hence, in future work, we will explore more advanced simulator tuning methods for more sample-efficient simulator tuning and robust Sim2Real policy transfer [2, 12, 42, 43]. The presented framework also must be rerun for each cable, motivating meta-learning [13] approaches to rapidly adapt to other cables.

ACKNOWLEDGMENTS

This research was performed at the AUTOLAB at UC Berkeley in affiliation with the Berkeley AI Research (BAIR) Lab and the CITRIS

“People and Robots” (CPAR) Initiative. The authors were supported in part by the Toyota Research Institute. We thank our colleagues Justin Kerr, Alejandro Escontrela, Ashwin Balakrishna, Ellen Novoseller, Brijen Thananjeyan, Harry Zhang, Zachary Tam, Chung Min Kim, and Ananth Rao for helpful comments.

REFERENCES

- [1] J. Achiam, *Spinning Up in Deep Reinforcement Learning*, 2018.
- [2] A. Allevato, E. S. Short, M. Pryor, and A. Thomaz, “Tunenet: One-shot residual tuning for system identification and sim-to-real robot task transfer,” in *Conference on Robot Learning*, PMLR, 2020, pp. 445–455.
- [3] T. G. authors, *Gpyopt: A bayesian optimization framework in python*, <http://github.com/SheffieldML/GPyOpt>, 2016.
- [4] K. Bathe, *Finite Element Procedures*. Prentice Hall, 2006.
- [5] J. van den Berg, S. Miller, D. Duckworth, H. Hu, A. Wan, X.-Y. Fu, K. Goldberg, and P. Abbeel, “Superhuman Performance of Surgical Tasks by Robots Using Iterative Learning from Human-Guided Demonstrations,” in *IEEE International Conference on Robotics and Automation (ICRA)*, 2010.
- [6] G. Bradski, “The OpenCV Library,” *Dr. Dobb’s Journal of Software Tools*, 2000.
- [7] P. Chang and T. Padir, “Sim2Real2Sim: Bridging the Gap Between Simulation and Real-World in Flexible Object Manipulation,” in *IEEE International Conference on Robotic Computing (IRC)*, 2020.
- [8] Y. Chebotar, A. Handa, V. Makovychuk, M. Macklin, J. Issac, N. Ratliff, and D. Fox, “Closing the Sim-to-Real Loop: Adapting Simulation Randomization with Real World Experience,” in *IEEE International Conference on Robotics and Automation (ICRA)*, 2019.
- [9] J. Collins, R. Brown, J. Leitner, and D. Howard, “Traversing the Reality Gap via Simulator Tuning,” *arXiv preprint arXiv:2003.01369*, 2020.
- [10] E. Coumans and Y. Bai, *PyBullet, a Python Module for Physics Simulation for Games, Robotics and Machine Learning*, <http://pybullet.org>, 2021.
- [11] F. von Drigalski, D. Joshi, T. Murooka, K. Tanaka, M. Hamaya, and Y. Ijiri, “An Analytical Diabolo Model for Robotic Learning and Control,” *arXiv preprint arXiv:2011.09068*, 2020.
- [12] Y. Du, O. Watkins, T. Darrell, P. Abbeel, and D. Pathak, “Auto-Tuned Sim-to-Real Transfer,” in *IEEE International Conference on Robotics and Automation (ICRA)*, 2021.
- [13] C. Finn, P. Abbeel, and S. Levine, “Model-Agnostic Meta-Learning for Fast Adaptation of Deep Networks,” in *International Conference on Machine Learning (ICML)*, 2017.
- [14] P. I. Frazier, “A tutorial on bayesian optimization,” *arXiv preprint arXiv:1807.02811*, 2018.
- [15] C. Gatti-Bonoia and N. Perkins, “Numerical Model for the Dynamics of a Coupled Fly Line / Fly Rod System and Experimental Validation,” *Journal of Sound and Vibration*, 2004.
- [16] J. Grannen, P. Sundaresan, B. Thananjeyan, J. Ichnowski, A. Balakrishna, M. Hwang, V. Viswanath, M. Laskey, J. E. Gonzalez, and K. Goldberg, “Untangling Dense Knots by Learning Task-Relevant Keyoints,” in *Conference on Robot Learning (CoRL)*, 2020.
- [17] J. Hopcroft, J. Kearney, and D. Krafft, “A Case Study of Flexible Object Manipulation,” in *International Journal of Robotics Research (IJRR)*, 1991.
- [18] J. Ibarz, J. Tan, C. Finn, M. Kalakrishnan, P. Pastor, and S. Levine, “How to Train Your Robot with Deep Reinforcement Learning: Lessons we Have Learned,” in *International Journal of Robotics Research (IJRR)*, 2021.
- [19] J. Ichnowski, Y. Avigal, V. Satish, and K. Goldberg, “Deep learning can accelerate grasp-optimized motion planning,” *Science Robotics*, vol. 5, no. 48, 2020.
- [20] N. Jakobi, P. Husbands, and I. Harvey, “Noise and the Reality Gap: The use of Simulation in Evolutionary Robotics,” in *European Conference on Advances in Artificial Life*, 1995.
- [21] S. Kim, A. Shukla, and A. Billard, “Catching Objects in Flight,” *IEEE Transactions on Robotics*, vol. 30, no. 5, pp. 1049–1065, 2014.
- [22] Y.-H. Kim and D. A. Shell, “Using a Compliant, Unactuated Tail to Manipulate Objects,” in *IEEE Robotics and Automation Letters (RA-L)*, 2016.
- [23] S. M. LaValle and J. J. Kuffner, “Randomized Kinodynamic Planning,” in *International Journal of Robotics Research (IJRR)*, 2001.
- [24] X. Lin, Y. Wang, J. Olkin, and D. Held, “SoftGym: Benchmarking Deep Reinforcement Learning for Deformable Object Manipulation,” in *Conference on Robot Learning (CoRL)*, 2020.
- [25] D. J. Lizotte, T. Wang, M. H. Bowling, D. Schuurmans, et al., “Automatic gait optimization with gaussian process regression,” in *IJCAI*, vol. 7, 2007, pp. 944–949.
- [26] L. Ljung, *System Identification: Theory for the User*. USA: Prentice-Hall, Inc., 1986.
- [27] T. Lopez-Guevara, R. Pucci, N. K. Taylor, M. U. Gutmann, S. Ramamoorthy, and K. Suhr, “Stir to pour: Efficient calibration of liquid properties for pouring actions,” in *2020 IEEE/RSJ International Conference on Intelligent Robots and Systems (IROS)*, 2020, pp. 5351–5357.
- [28] W. H. Lui and A. Saxena, “Tangled: Learning to Untangle Ropes with RGB-D Perception,” in *IEEE/RSJ International Conference on Intelligent Robots and Systems (IROS)*, 2013.
- [29] K. M. Lynch and M. T. Mason, “Dynamic nonprehensile manipulation: Controllability, planning, and experiments,” *The International Journal of Robotics Research*, vol. 18, no. 1, pp. 64–92, 1999.
- [30] M. Macklin, M. Muller, N. Chentanez, and T.-Y. Kim, “Unified Particle Physics for Real-Time Applications,” *ACM Trans. Graph.*, vol. 33, no. 4, Jul. 2014.
- [31] J. Mahler, J. Liang, S. Niyaz, M. Laskey, R. Doan, X. Liu, J. A. Ojea, and K. Goldberg, “Dex-Net 2.0: Deep Learning to Plan Robust Grasps with Synthetic Point Clouds and Analytic Grasp Metrics,” in *Robotics: Science and Systems (RSS)*, 2017.
- [32] V. Makovychuk, L. Wawrzyniak, Y. Guo, M. Lu, K. Storey, M. Macklin, D. Hoeller, N. Rudin, A. Allshire, A. Handa, and G. State, *Isaac Gym: High Performance GPU-Based Physics Simulation For Robot Learning*, 2021. arXiv: 2108.10470 [cs.LG].
- [33] M. T. Mason and K. M. Lynch, “Dynamic Manipulation,” in *IEEE/RSJ International Conference on Intelligent Robots and Systems (IROS)*, 1993.
- [34] J. Matas, S. James, and A. J. Davison, “Sim-to-Real Reinforcement Learning for Deformable Object Manipulation,” *Conference on Robot Learning (CoRL)*, 2018.
- [35] H. Mayer, F. Gomez, D. Wierstra, I. Nagy, A. Knoll, and J. Schmidhuber, “A System for Robotic Heart Surgery that Learns to Tie the Knots Using Recurrent Neural Networks,” in *IEEE/RSJ International Conference on Intelligent Robots and Systems (IROS)*, 2006.
- [36] T. Morita, J. Takamatsu, K. Ogawara, H. Kimura, and K. Ikeuchi, “Knot Planning from Observation,” in *IEEE International Conference on Robotics and Automation (ICRA)*, 2003.
- [37] M. Mukadam, J. Dong, X. Yan, F. Dellaert, and B. Boots, “Continuous-time Gaussian Process Motion Planning via Probabilistic Inference,” in *International Journal of Robotics Research (IJRR)*, 2018.
- [38] A. Nair, D. Chen, P. Agrawal, P. Isola, P. Abbeel, J. Malik, and S. Levine, “Combining Self-Supervised Learning and Imitation for Vision-Based Rope Manipulation,” in *IEEE International Conference on Robotics and Automation (ICRA)*, 2017.
- [39] H. Nakagaki, K. Kitagi, T. Ogasawara, and H. Tsukune, “Study of Deformation and Insertion Tasks of Flexible Wire,” in *IEEE International Conference on Robotics and Automation (ICRA)*, 1997.
- [40] Y. Narang, Y. Li, M. Macklin, D. McConachie, and J. Wu, *RSS 2021 Workshop on Deformable Object Simulation in Robotics*, <https://sites.google.com/nvidia.com/do-sim>, Accessed: 2021-09-12.
- [41] D. Pathak, P. Mahmoudieh, G. Luo, P. Agrawal, D. Chen, Y. Shentu, E. Shelhamer, J. Malik, A. A. Efros, and T. Darrell, “Zero-Shot Visual Imitation,” in *International Conference on Learning Representations (ICLR)*, 2018.
- [42] X. B. Peng, M. Andrychowicz, W. Zaremba, and P. Abbeel, “Sim-to-Real Transfer of Robotic Control with Dynamics Randomization,” in *IEEE International Conference on Robotics and Automation (ICRA)*, 2018.
- [43] F. Ramos, R. Possas, and D. Fox, “Bayessim: Adaptive domain randomization via probabilistic inference for robotics simulators,” in *Proceedings of Robotics: Science and Systems, Freiburg/Breisgau, Germany*, Jun. 2019.

- [44] C. Rasmussen and C. Williams, *Gaussian Processes for Machine Learning*. MIT Press, 2006.
- [45] F. Ruiz-Ugalde, G. Cheng, and M. Beetz, “Fast adaptation for effect-aware pushing,” in *2011 11th IEEE-RAS International Conference on Humanoid Robots*, IEEE, 2011, pp. 614–621.
- [46] F. Sadeghi and S. Levine, “CAD2RL: Real Single-Image Flight without a Single Real Image,” in *Robotics: Science and Systems (RSS)*, 2017.
- [47] J. Sanchez, J.-A. Corrales, B.-C. Bouzgarrou, and Y. Mezouar, “Robotic Manipulation and Sensing of Deformable Objects in Domestic and Industrial Applications: a Survey,” in *International Journal of Robotics Research (IJRR)*, 2018.
- [48] D. Seita, P. Florence, J. Tompson, E. Coumans, V. Sindhwani, K. Goldberg, and A. Zeng, “Learning to Rearrange Deformable Cables, Fabrics, and Bags with Goal-Conditioned Transporter Networks,” in *IEEE International Conference on Robotics and Automation (ICRA)*, 2021.
- [49] S. Sen, A. Garg, D. V. Gealy, S. McKinley, Y. Jen, and K. Goldberg, “Automating Multi-Throw Multilateral Surgical Suturing with a Mechanical Needle Guide and Sequential Convex Optimization,” in *IEEE International Conference on Robotics and Automation (ICRA)*, 2016.
- [50] B. Shahriari, K. Swersky, Z. Wang, R. P. Adams, and N. De Freitas, “Taking the human out of the loop: A review of bayesian optimization,” *Proceedings of the IEEE*, vol. 104, no. 1, pp. 148–175, 2015.
- [51] Y. She, S. Dong, S. Wang, N. Sunil, A. Rodriguez, and E. Adelson, “Cable Manipulation with a Tactile-Reactive Gripper,” in *Robotics: Science and Systems (RSS)*, 2020.
- [52] R. Storn and K. Price, “Differential evolution—a simple and efficient heuristic for global optimization over continuous spaces,” *Journal of global optimization*, vol. 11, no. 4, pp. 341–359, 1997.
- [53] J. Tobin, R. Fong, A. Ray, J. Schneider, W. Zaremba, and P. Abbeel, “Domain Randomization for Transferring Deep Neural Networks from Simulation to the Real World,” in *IEEE/RSJ International Conference on Intelligent Robots and Systems (IROS)*, 2017.
- [54] P. Virtanen, R. Gommers, T. E. Oliphant, M. Haberland, T. Reddy, D. Cournapeau, E. Burovski, P. Peterson, W. Weckesser, J. Bright, S. J. van der Walt, M. Brett, J. Wilson, K. J. Millman, N. Mayorov, A. R. J. Nelson, E. Jones, R. Kern, E. Larson, C. J. Carey, Í. Polat, Y. Feng, E. W. Moore, J. VanderPlas, D. Laxalde, J. Perktold, R. Cimrman, I. Henriksen, E. A. Quintero, C. R. Harris, A. M. Archibald, A. H. Ribeiro, F. Pedregosa, P. van Mulbregt, and SciPy 1.0 Contributors, “SciPy 1.0: Fundamental Algorithms for Scientific Computing in Python,” *Nature Methods*, vol. 17, pp. 261–272, 2020.
- [55] C. Wang, S. Wang, B. Romero, F. Veiga, and E. Adelson, “Swing-Bot: Learning Physical Features from In-hand Tactile Exploration for Dynamic Swing-up Manipulation,” in *IEEE/RSJ International Conference on Intelligent Robots and Systems (IROS)*, 2020.
- [56] G. Wang and N. Wereley, “Analysis of Fly Fishing Rod Casting Dynamics,” *Shock and Vibration*, vol. 18, no. 6, pp. 839–855, 2011.
- [57] W. Wang and D. Balkcom, “Tying Knot Precisely,” in *IEEE International Conference on Robotics and Automation (ICRA)*, 2016.
- [58] W. Wang, D. Berenson, and D. Balkcom, “An Online Method for Tight-Tolerance Insertion Tasks for String and Rope,” in *IEEE International Conference on Robotics and Automation (ICRA)*, 2015.
- [59] Y. Wu, W. Yan, T. Kurutach, L. Pinto, and P. Abbeel, “Learning to Manipulate Deformable Objects without Demonstrations,” in *Robotics: Science and Systems (RSS)*, 2020.
- [60] Y. Yamakawa, A. Namiki, and M. Ishikawa, “Motion Planning for Dynamic Knotting of a Flexible Rope With a High-Speed Robot Arm,” in *IEEE/RSJ International Conference on Intelligent Robots and Systems (IROS)*, 2010.
- [61] —, “Simple Model and Deformation Control of a Flexible Rope Using Constant, High-speed Motion of a Robot Arm,” in *IEEE International Conference on Robotics and Automation (ICRA)*, 2012.
- [62] —, “Dynamic High-Speed Knotting of a Rope by a Manipulator,” in *International Journal of Advanced Robotic Systems*, 2013.
- [63] Y. Yamakawa, A. Namiki, M. Ishikawa, and M. Shimojo, “One-Handed Knotting of a Flexible Rope With a High-Speed Multifingered Hand Having Tactile Sensors,” in *IEEE/RSJ International Conference on Intelligent Robots and Systems (IROS)*, 2007.
- [64] W. Yan, A. Vangipuram, P. Abbeel, and L. Pinto, “Learning Predictive Representations for Deformable Objects Using Contrastive Estimation,” in *Conference on Robot Learning (CoRL)*, 2020.
- [65] A. Zeng, P. Florence, J. Tompson, S. Welker, J. Chien, M. Attarian, T. Armstrong, I. Krasin, D. Duong, V. Sindhwani, and J. Lee, “Transporter Networks: Rearranging the Visual World for Robotic Manipulation,” in *Conference on Robot Learning (CoRL)*, 2020.
- [66] A. Zeng, S. Song, J. Lee, A. Rodriguez, and T. Funkhouser, “TossingBot: Learning to Throw Arbitrary Objects with Residual Physics,” in *Robotics: Science and Systems (RSS)*, 2019.
- [67] H. Zhang, J. Ichnowski, D. Seita, J. Wang, and K. Goldberg, “Robots of the Lost Arc: Learning to Dynamically Manipulate Fixed-Endpoint Ropes and Cables,” in *IEEE International Conference on Robotics and Automation (ICRA)*, 2021.
- [68] S. Zimmermann, R. Poranne, and S. Coros, “Dynamic Manipulation of Deformable Objects with Implicit Integration,” in *IEEE Robotics and Automation Letters (RA-L)*, 2021.